



Portable Bridge Weigh-In-Motion (P-B-WIM)

Yahya M. Mohammed¹, Nasim Uddin², Chengjun Tan³, and Zhenhua Shi⁴

^{1,3,4} Ph.D. Student, Department of Civil Construction and Environmental Engineering, University of Alabama at Birmingham, Birmingham, AL, 35294, USA.

Emails: yahya1@uab.edu

²Ph.D., P.E., Professor, Department of Civil Construction and Environmental Engineering, University of Alabama at Birmingham, Birmingham, AL, 35294, USA. Email: nuddin@uab.edu.

Abstract

Bridge Weigh-in-Motion (B-WIM) is the concept of using measured strains on a bridge to calculate the axle weights of trucks as they pass overhead at full highway speed. There exist a consensus that conventional instrumentation faces substantial practical problems that halts the feasibility of this theory, namely cost, installation time and complexity. This article will go through a new concept by moving toward the first Portable Bridge Weigh-In-Motion (P-B-WIM) system. The system introduce flying sensor concept which consist of a swarm of drones that have accelerometers and able to latch bridge girders to record acceleration data. Some perching mechanisms have been introduce in this paper to allow drones to latch bridges girders. At the same time, a new algorithm is developed to allow the B-WIM system to use the acceleration data to estimate the truck weigh instead of the strain measurements. The algorithm uses the kalman-filter-based estimation algorithm to estimate the state vectors (displacement and velocities) using limited measured acceleration response (from drones). The estimated state vector is used to feed a moving force identification (MFI) algorithm that shows good results in estimating a quarter car model weight.

Keywords: Acceleration, B-WIM, Kalman Filter, Strain, Measurements, Portable, Drone, UAV.

1. Introduction

The axle load and gross weight of vehicles are important information for the design of new bridges and pavements, the rating and fatigue life assessments of existing bridges and pavements, design code calibration and the control of overweight vehicles to highway regulations (Asnachinda, Pinkaew et al. 2008). Therefore, the dynamic moving forces produced by the vehicles on the bridge structure must be determined by adopting the estimation method or measurement techniques. In the late 1970s in the United States, Moses (Moses 1979) first introduced the Bridge Weigh-In-Motion (B-WIM) system, which is the concept of using measured strains on a bridge to calculate the axle weights as they pass overhead at full highway speed. Then Zhu, and Law extend the theory for the multi-span continuous bridge (Zhu and Law 1999). In more recent years, the field of moving force identification (MFI) has been developed by Chan, Law, and others (Chan and O'Connor 1990, Chan, Law et al. 2000, Law and Fang 2001, Jiang, Au et al. 2003, Pinkaew 2006, Mohammed and Uddin 2017, Mohammed and Uddin

2018, Mohammed and Uddin 2018, Mohammed and Uddin 2018). Law and Fang (Law and Fang 2001) have applied the dynamic programming method to the MFI problem using zero order regularization. Then González (González, Rowley et al. 2008) extended the algorithm with first order regularization, which improved the solution accuracy (O'Brien, Znidaric et al. 2008, Rowley, O'Brien et al. 2009). Recently, Mohammed (Mohammed, Uddin et al. 2019) reduced the algorithm computational time specially when using 3D bridge models which allow for real time B-WIM system.

The main drawback of the B-WIM system is the installation time and cost, especially for the high elevation bridges, which need huge equipment and trained labors to install strain sensors. A wide variety of engineering applications employ acceleration to identify desired information because acceleration sensors are generally cost-effective, convenient to install, have relatively low noise (Park, Sim et al. 2013), and recently can easily attach to the bridge girders using drones (Na and Baek 2016) .

In this study, a possible application concept of UAV, combined with a vibration-based non-destructive health monitoring method, is proposed. The idea is the accelerometer will be inserted on the drone which temporarily will attach onto a specific region of the bridge to collect the vibration data. Then, a procedure is developed to estimate the moving loads on bridges using limited measured acceleration responses. This system will be called Portable B-WIM system.

1 Perching Mechanisms

There are several perching mechanisms that have been proposed the last few years, Hawkes (Hawkes, Christensen et al. 2013, Jiang, Pope et al. 2014, Hawkes 2017) proposes a perching mechanism for micro air vehicles (MAVs) that allow perching for wall or ceiling using directional adhesive. The perching mechanism used in this study is consist of double- sided restickable tab Figure 1-a, which allow small drone to attach on the bridge just for one or two times (Figure 1-c). This tape measures 25.4 x25.4 mm, the thickness of 2mm, and is suitable for bonding with many kinds of material with a flat surface like wood, metals, etc.

The drone used in this paper is called Crazyflie 2.0 (Figure 1-b) manufactured by Bitcraze. Crazyflie 2.0 is a versatile open source flying development platform that fits in the palm of your hand. Crazyflie 2.0 is equipped with low-latency/long-range radio as well as Bluetooth LE. The drone can be controlled by user mobile device or it can be programed to reach specific location.

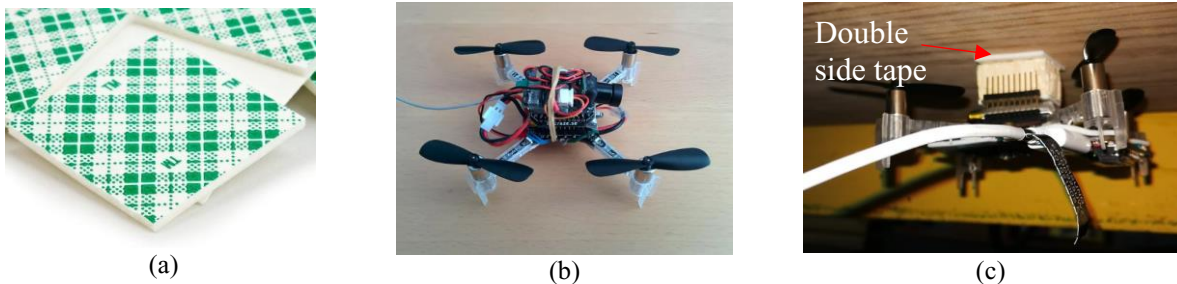


Figure 1. (a) Double side tape, (b) Light weight drone, and (c) Drone attaching to wood.

2 Accelerometer Performance

To test the accelerometer performance when inserted on a drone and the drone has been attaching on a bridge, a free vibration test on the simply supported wood bridge has been performed. The bridge has 2.40 m span and cross section of 0.235m x 0.04m. The accelerometer used in this study has 500 HZ scanning frequency (Figure 2-a). A comparison between two cases has been studied; the first case, the accelerometer has been install at the bridge mid-span and the acceleration data due to free vibration test has been collected. The second case, the same accelerometer has inserted on the drone and the drone has attached to the same bridge mid-span to collect the vibration data Figure 2-b. The FFT for both cases has been shown that the two cases have detected the same first bridge frequency which is 14.57 HZ (Figure 2-c). It should be noted that, for this experiment and after the drone has been attached on the bridge it wired to a computer to transfer the acceleration data.

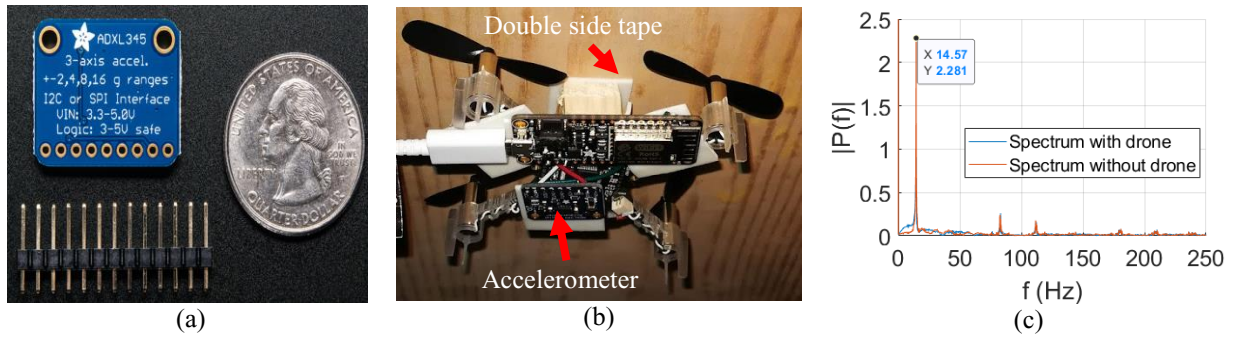


Figure 2. (a) Accelerometer, (b) Drone attach to the wood bridge and carry the accelerometer, and (c) Frequency spectrum for the acceleration collect for the drone case and without drone case.

3. Moving Force Identification (MFI) Algorithm using Acceleration Data

The main idea to use acceleration data instead of strain data to estimate the moving force is to use kalman-filter-based estimation algorithm to estimate the state vector (displacements and velocities), and then applying the MFI algorithm to estimate the moving forces.

2.1 STRUCTURAL RESPONSE ESTIMATION USING KALMAN FILTER

2.1.1 State space equation

The force-induced vibration of a bridge can be represented by the following equation of motion:

$$M\ddot{U} + C\dot{U} + KU = F \quad (1)$$

Where U , \dot{U} , and \ddot{U} denote the vectors of displacement, velocity, and acceleration, respectively. M , C , and K are the bridge mass matrix, damping matrix, and stiffness matrix, respectively. F is the time history vector of vehicle load. Using the modal response of sttthe ructure, Equation (1) can be transformed to modal space (Equation(2)).

$$\ddot{Z}_i + 2\xi_i\omega_i\dot{Z}_i + \omega_i^2Z_i = \Phi_i^T F = f_i \quad (i=1,2, \dots, N) \quad (2)$$

Where Φ_i denoted the modal shape of the i th mode. Z_i , \dot{Z}_i , \ddot{Z}_i , and f_i are the modal displacement, velocity, acceleration and moving force of the i th mode, respectively. N is the total number of modes, ξ_i , and ω_i are the damping ration and natural frequency of the i the mode. The modal acceleration response can be approximately calculated from limited measured acceleration response using the pseudoinverse of the mode shape matrix (Equation (3)).

$$\ddot{Z}_{qx1} = (\Phi_{pxq})^+ \ddot{U}_{px1} \quad (3)$$

Where P denotes the number of measurements, and q is the number of modes considered. The error between the exact and estimated modal acceleration responses can be minimized by choosing the measurements number P exceeding the number of modes governing the structural responses (Hwang, Kareem et al. 2009).

In the modal space, the state space equation and the modal output (Y) obtained from the acceleration response can be represented using Equation (4).

$$\dot{\lambda}_i(t) = A_i \lambda_i(t) + B_i f_i \quad (4.1)$$

$$Y_i(t) = H_i \lambda_i(t) + D_i f_i \quad (4.2)$$

Where the system matrix A_i , λ_i , f_i and B_i are

$$A_i = \begin{bmatrix} 0 & 1 \\ -\frac{K_i}{M_i} & -\frac{C_i}{M_i} \end{bmatrix} = \begin{bmatrix} 0 & 1 \\ -\omega_i^2 & -2\xi_i\omega_i \end{bmatrix}, \quad \lambda_i = [Z_i \quad \dot{Z}_i]^T, \quad f_i = \frac{F_i}{M_i}, \quad B_i = [0 \quad 1]^T$$

For acceleration measurements, H_i and D_i matrices are defined as $[-\omega_i^2 \quad -2\xi_i\omega_i]$, and $[1]$ respectively. Equation (4), discretized over time intervals of length Δt (Equation (5)).

$$\lambda_i(t+1) = \Psi_i \lambda_i(t) + \Gamma_i f_i(t) \quad (5.1)$$

$$Y_i(t) = H \lambda_i(t) + D_i f_i(t) \quad (5.2)$$

Where Ψ_i denotes the state transition matrix and equal to $e^{A_i\Delta t}$. Γ_i represents the process noise matrix and can be calculated using equation (6).

$$\Gamma_i = [\Psi_i - I]A_i^{-1}B_i \quad (6)$$

2.1.2. State Vector estimation using Kalman Filter

Based on the Kalman filter for the discrete-time state space system of Equations (5), the state vector $\lambda_i(t)$ can be estimated by the following equations (Equations 7-12) (Chui and Chen 1989, Simon 2006, Bell 2010).

$$\hat{\lambda}(t/t-1) = \Psi \hat{\lambda}(t-1) + J(t-1)[Y(t-1) - H \hat{\lambda}(t-1)] \quad (7)$$

$$\hat{\lambda}(t) = \hat{\lambda}(t/t-1) + G(t)[Y(t) - H \hat{\lambda}(t/t-1)] \quad (8)$$

$$J(t-1) = \Gamma Q(t-1)D^T[DQ(t-1)D^T + R(t-1)]^{-1} \quad (9)$$

$$P(t/t-1) = [\Psi - J(t-1)H]P(t-1) [\Psi - J(t-1)H]^T + \Gamma Q(t-1) \Gamma^T - J(t-1)DQ(t-1) \Gamma^T \quad (10)$$

$$G(t) = P(t/t-1)H[HP(t/t-1)H^T + DQ(t)D^T + R(t)]^{-1} \quad (11)$$

$$P(t) = [I - G(t)H]P(t/t-1) \quad (12)$$

where $G(t)$ is the Kalman filter gain matrix at time instant t . $P(t)$ denotes the filter's error covariance matrix, $J(t)$ is the a priori gain matrix.

The displacement and velocities time history (state vector) are identified as

$$U_{nx1} = \phi_{nxq} \hat{Z}_{qx1} \quad (17)$$

$$\dot{U}_{nx1} = \phi_{nxq} \dot{\hat{Z}}_{qx1} \quad (18)$$

Where n is the number of estimated DOFs.

2.1 Moving Force Identification (MFI) Algorithm

The algorithm adopted in this paper is that used by González et al. (González, Rowley et al. 2008) who improve the work of Law et al. (Law and Fang 2001) by applying the first-order regularization technique.

The change in the moving force $\{r\}_j$ can be define from the following last square minimization with Tikhonov regularization (Equation (19)).

$$\sum_{j=1}^m (\{\{d_{me}\}_j - [Q]\{X\}_j\}, [W]\{\{d_{me}\}_j - [Q]\{X\}_j\} + \{r\}_j, [B]\{r\}_j) \quad (19)$$

where d_{me} is the measurement vector (usually strain), $[Q]$ is a vector to relate the measurements to the degree of freedom, (x, y) denotes the vector product of x and y , $[W]$ is an $m \times m$ identity matrix in the least squares error. $[B]$ is a regularized matrix equal to $\lambda[I]$, where λ is the optimum regularization parameter, and its value is usually obtained using the L-curve method (Hansen 1992, Hansen 1994, Lawson and Hanson 1995, Hansen 2005). It should be mentioned that the MFI algorithm require a calibrated FE model.

3 Numerical Simulation

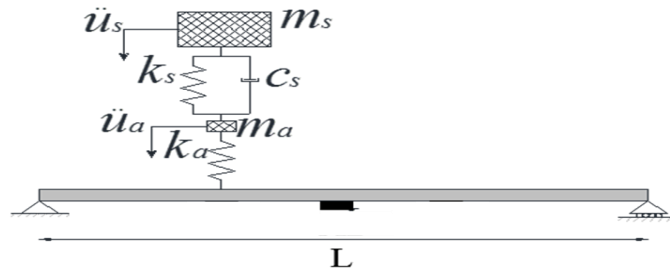


Figure 3. Theoretical quarter car model on simply supported beam

As shown in Figure 3, a simply supported bridge subject to a moving quarter-car model is taken as an example for numerical simulation. The quarter-car travels with the constant speed of 15.0 m/s crossing a 20-m approach distance followed by a 15-m simply supported finite element (FE) bridge. The bridge is modeled with 1D Euler–Bernoulli finite beam elements with two degrees of freedom per node, vertical translation, and rotation. The vehicle masses are represented by a sprung mass, m_s , and un-sprung mass, m_a represents the vehicle axle mass and body mass respectively. The Degrees of Freedoms (DOFs) that correspond to the bouncing of the sprung and the axle masses are, u_s , and u_a , respectively. The properties of the quarter-car and the bridge are listed in Table 1 and based upon the work of Cebon (1999) and Harris, OBrien et al. (2007). The dynamic interaction between the vehicle and the bridge that showing how bridge and vehicle

properties affect the response is implemented in MATLAB (Elhatab, Uddin et al. 2015, Elhatab, Uddin et al. 2016, Mohammed and Uddin 2019) based on the contact force concept adopted by Yang et al (Yang, Yau et al. 2004). and Gonzalez (González 2010). Unless otherwise mentioned, the used scanning frequency is 1000 Hz. The acceleration response at the bridge mid-span has been extracted and plotted in Figure 4-a. the estimated displacement at the bridge mid-span vs. the actual displacement is plotted in Figure 4-b. the estimated displacement has been used as input to the MFI algorithm and the force history has been plotted to compare with the actual force in Figure 4-c.

Table 1. Vehicle and Bridge properties.

Vehicle properties		Bridge properties	
ms	14000 kg	Span	15m
ma	1000 kg	Density	4800 kg/m ³
k _s	2e5 N/m	Width	4.0 m
K _a	2.75e6 N/m	Depth	0.8 m
c _a	1e4 N s/m	Modulus	2.75×10 ¹⁰ N/m ²

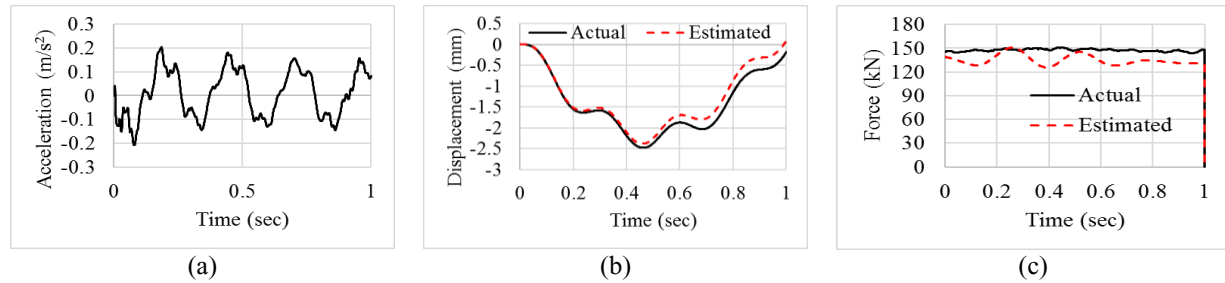


Figure 4. (a) Acceleration at mid-span, (b) estimated vs. actual displacement using the kalman filter, and (c) actual vs. estimated force history.

4 Conclusion

In conclusion, this paper proposes a portable B-WIM system. The system is mainly focused on: firstly; replacing the strain measurements with the acceleration ones as the main input to the B-WIM algorithm. Secondly, insert accelerometers in the drone and use it as flying sensors that can attach to the bridge. In this paper a simple perching mechanism has been tested and proven a good catching to the bridge frequency. Also, a new Moving force Identification algorithm has been developed based on the kalman-filter-based estimation algorithm to use the acceleration measurements instead of the strain to calculate the weight of the moving vehicle.

5 Acknowledgments

The authors would like to express their gratitude for the financial support received from the National Science Foundation (NSF-CNS- 1645863, and NSF-CSR- 1813949) for this investigation.

6 References

Asnachinda, P., T. Pinkaew and J. Laman (2008). "Multiple vehicle axle load identification from continuous bridge bending moment response." *Engineering Structures* **30**(10): 2800-2817.

- Bell, B. M. (2010). Kalman Filtering with Real-Time Applications, JSTOR.
- Cebon, D. (1999). Handbook of vehicle-road interaction.
- Chan, T. H., S. Law and T. Yung (2000). "Moving force identification using an existing prestressed concrete bridge." Engineering Structures **22**(10): 1261-1270.
- Chan, T. H. T. and C. O'Connor (1990). "Wheel loads from highway bridge strains: field studies." Journal of structural engineering **116**(7): 1751-1771.
- Chui, C. and G. Chen (1989). "Kalman filtering with real time applications." Applied Optics **28**: 1841.
- Elhattab, A., N. Uddin and E. Obrien (2015). "DRIVE-BY BRIDGE DAMAGE DETECTION USING APPARENT PROFILE." First International Conference on Advances in Civil Infrastructure and Construction Materials (CISM): 33-45.
- Elhattab, A., N. Uddin and E. OBrien (2016). "Drive-by bridge damage monitoring using Bridge Displacement Profile Difference." Journal of Civil Structural Health Monitoring **6**(5): 839-850.
- González, A. (2010). Vehicle-bridge dynamic interaction using finite element modelling. Finite element analysis, InTech.
- González, A., C. Rowley and E. J. OBrien (2008). "A general solution to the identification of moving vehicle forces on a bridge." International journal for numerical methods in engineering **75**(3): 335-354.
- Hansen, P. C. (1992). "Analysis of discrete ill-posed problems by means of the L-curve." SIAM review **34**(4): 561-580.
- Hansen, P. C. (1994). "Regularization tools: A Matlab package for analysis and solution of discrete ill-posed problems." Numerical algorithms **6**(1): 1-35.
- Hansen, P. C. (2005). Rank-deficient and discrete ill-posed problems: numerical aspects of linear inversion, Siam.
- Harris, N. K., E. J. OBrien and A. González (2007). "Reduction of bridge dynamic amplification through adjustment of vehicle suspension damping." Journal of Sound and Vibration **302**(3): 471-485.
- Hawkes, E. W. (2017). Surface grasping mechanism using directional adhesives, Google Patents.
- Hawkes, E. W., D. L. Christensen, E. V. Eason, M. A. Estrada, M. Heverly, E. Hilgemann, H. Jiang, M. Pope, A. Parness and M. R. Cutkosky (2013). Dynamic surface grasping with directional adhesion. IROS.
- Hwang, J.-s., A. Kareem and W.-j. Kim (2009). "Estimation of modal loads using structural response." Journal of Sound and Vibration **326**(3-5): 522-539.
- Jiang, H., M. T. Pope, E. W. Hawkes, D. L. Christensen, M. A. Estrada, A. Parlier, R. Tran and M. R. Cutkosky (2014). Modeling the dynamics of perching with opposed-grip mechanisms. Robotics and Automation (ICRA), 2014 IEEE International Conference on, IEEE.
- Jiang, R., F. Au and Y. Cheung (2003). "Identification of masses moving on multi-span beams based on a genetic algorithm." Computers & structures **81**(22): 2137-2148.
- Law, S. and Y. Fang (2001). "Moving force identification: optimal state estimation approach." Journal of Sound and Vibration **239**(2): 233-254.
- Lawson, C. L. and R. J. Hanson (1995). Solving least squares problems, Siam.
- Mohammed, Y. M. and N. Uddin (2017). Bridge Damage Detection using the Inverse Dynamics Optimization Algorithm. 26th ASNT Research Symposium.
- Mohammed, Y. M. and N. Uddin (2018). "B-WIM SYSTEM USING FEWER SENSORS." Transportation Management.

- Mohammed, Y. M. and N. Uddin (2018). Field Verification for B-WIM System using Wireless Sensors. 27th ASNT Research Symposium.
- Mohammed, Y. M. and N. Uddin (2018). Passenger Vehicle Effect on the Truck Weight Calculations using B-WIM System. 27th ASNT Research Symposium.
- Mohammed, Y. M. and N. Uddin (2019). "Acceleration-based bridge weigh-in-motion." Bridge Structures.
- Mohammed, Y. M., N. Uddin and E. J. OBrien (2019). "Moving force identification for real-time bridge weigh-in-motion." Bridge Structures.
- Moses, F. (1979). "Weigh-in-motion system using instrumented bridges." Journal of Transportation Engineering **105**(3).
- Na, W. S. and J. Baek (2016). "Impedance-based non-destructive testing method combined with unmanned aerial vehicle for structural health monitoring of civil infrastructures." Applied Sciences **7**(1): 15.
- O'Brien, E., A. Znidaric and T. Ojio (2008). Bridge weigh-in-motion—Latest developments and applications world wide. Proceedings of the International Conference on Heavy Vehicles, Paris, France: John Wiley.
- Park, J.-W., S.-H. Sim and H.-J. Jung (2013). "Development of a wireless displacement measurement system using acceleration responses." Sensors **13**(7): 8377-8392.
- Pinkaew, T. (2006). "Identification of vehicle axle loads from bridge responses using updated static component technique." Engineering Structures **28**(11): 1599-1608.
- Rowley, C., E. J. OBrien, A. González and A. Žnidarič (2009). "Experimental testing of a moving force identification bridge weigh-in-motion algorithm." Experimental Mechanics **49**(5): 743-746.
- Simon, D. (2006). Optimal state estimation: Kalman, H infinity, and nonlinear approaches, John Wiley & Sons.
- Yang, Y.-B., J. Yau, Z. Yao and Y. Wu (2004). Vehicle-bridge interaction dynamics: with applications to high-speed railways, World Scientific.
- Zhu, X. and S. Law (1999). "Moving forces identification on a multi-span continuous bridge." Journal of sound and vibration **228**(2): 377-396.